

# Modification of Ta/polymeric low-k interface by electron beam treatment

Prasad, K.; Damayanti, M.; Gan, Zhenghao; Mhaisalkar, Subodh Gautam; Chen, Zhong; Chen, Zhe; Zhang, Sam; Jiang, Ning

2006

Gan, Z., Mhaisalkar, S. G., Chen, Z., Chen, Z., Prasad, K., Zhang, S., et al. (2006). Modification of Ta/polymeric low-k interface by electron beam treatment. *Journal of the electrochemical society*, 153.

<https://hdl.handle.net/10356/90682>

<https://doi.org/10.1149/1.2129493>

---

© 2006 The Electrochemical Society. This paper was published in *Journal of The Electrochemical Society* and is made available as an electronic reprint (preprint) with permission of The Electrochemical Society. The paper can be found at the following DOI: <http://dx.doi.org/10.1149/1.2129493>. One print or electronic copy may be made for personal use only. Systematic or multiple reproduction, distribution to multiple locations via electronic or other means, duplication of any material in this paper for a fee or for commercial purposes, or modification of the content of the paper is prohibited and is subject to penalties under law.



## Modification of Ta/Polymeric Low- $k$ Interface by Electron-Beam Treatment

Zhenghao Gan,<sup>a,z</sup> S. G. Mhaisalkar,<sup>a</sup> Zhong Chen,<sup>a</sup> Zhe Chen,<sup>b</sup> K. Prasad,<sup>b</sup> Sam Zhang,<sup>c</sup> M. Damayanti,<sup>a</sup> and N. Jiang<sup>d</sup>

<sup>a</sup>School of Materials Science and Engineering, <sup>b</sup>School of Electrical and Electronic Engineering, and <sup>c</sup>School of Mechanical and Aerospace Engineering, Nanyang Technological University, Singapore 639798  
<sup>d</sup>Institute of Microelectronics, Singapore 117685

Polymeric dielectric, porous polyarylene ether (PAE), was introduced in the Cu damascene structures because of its low dielectric constant to reduce resistance-capacitance (RC) delay. One of the requirements of a low- $k$  material includes its good adhesion to the other interconnect materials. In the present study, the adhesion energy ( $G_c$ ) of the barrier layer Ta/PAE interface was quantitatively measured by a four-point bending technique. The obtained  $G_c$  value of the pristine Ta/PAE interface was  $5.9 \pm 1.1$  J/m<sup>2</sup>. If the PAE was subjected to electron-beam (EB) treatment with low dose ( $20 \mu\text{C}/\text{cm}^2$ ) prior to Ta deposition,  $G_c$  value increased to  $8.1 \pm 0.5$  J/m<sup>2</sup>. However, with high-dose ( $40 \mu\text{C}/\text{cm}^2$ ) EB treatment,  $G_c$  value reduced to  $4.0 \pm 0.6$  J/m<sup>2</sup>. The adhesion improvement and degradation induced by low- and high-dose EB were correlated to the increase and reduction of the amount of C–Ta bonds at the Ta/PAE interface, respectively. The phenomena were further studied by X-ray photoelectron spectroscopy analysis. © 2005 The Electrochemical Society. [DOI: 10.1149/1.2129493] All rights reserved.

Manuscript submitted June 19, 2005; revised manuscript received August 23, 2005. Available electronically November 10, 2005.

As the feature sizes continue to reduce in ultra large-scale integration (ULSI), on-chip interconnects are being scaled aggressively and the resistance-capacitance (RC) delay becomes a serious concern. According to the International Technology Roadmap for Semiconductors (ITRS) 2003,<sup>1</sup> as feature sizes in integrated circuits approach  $0.1 \mu\text{m}$ , it is necessary to reduce the dielectric constant of the dielectrics materials to below 2.2. This means these dielectric materials will need to be produced in a porous form.

Due to the inherent mechanical weakness of the low- $k$  material, adhesion of the low- $k$  material to the surrounding layers becomes a critical issue for application consideration in the back-end-of-line (BEOL), especially when the dielectric material is highly porous. One of the diverse requirements of a low- $k$  material in order to be successfully integrated includes its good adhesion to the other interconnect materials, because interfacial debonding of multilayer interconnect thin films can affect the reliability of electronic devices.<sup>2-6</sup>

Polymeric low- $k$  dielectric, porous polyarylene ether (PAE), was introduced in the Cu damascene structures because of its low dielectric constant (i.e.,  $k$ ) of 2.65 and high thermal stability ( $>425^\circ\text{C}$ ).<sup>7</sup> Another advantage is that it could be fabricated by the lower cost spin-on process, compared with the silicon-based chemical vapor deposition (CVD).<sup>8</sup> A metallic barrier layer Ta was employed to block Cu diffusion into the dielectric. However, the reliability issues, mostly associated with the poor electrical/mechanical properties of this kind of low- $k$  films, are major concerns in the Cu/organic low- $k$  damascene process.<sup>1</sup> It has been demonstrated previously that the film stack may delaminate during chemical mechanical polishing (CMP) if the interfacial adhesion energy ( $G_c$ ) value is less than  $5 \text{ J/m}^2$ .<sup>9</sup>

In the present study, the adhesion energy ( $G_c$ ) of the Ta/PAE interface was quantitatively measured by four-point bending technique. The interaction at the Ta/PAE interface was demonstrated by X-ray photoelectron spectroscopy (XPS) depth profile and detailed core-level spectra analysis. The effect of electron-beam (EB) treatment on the Ta/PAE interface adhesion is studied in-depth.

### Experimental

Figure 1 shows the thin-film stack to study the Ta/PAE interfacial adhesion strength. The thin-film stack was prepared on 8-in.-diam p-type Si(100) wafers. PAE layer with a thickness of 300 nm was first spun onto the wafer. After that, a 25-nm-thick Ta layer was deposited immediately by an Applied Materials high-density plasma physical vapor deposition (HD-PVD) system with self-ionized

plasma (SIP) technology. Two other wafers with PAE film were exposed under EB in a vacuum chamber by employing an EB scan/lithography system prior to Ta deposition. The doses for the EB exposure were  $20 \mu\text{C}/\text{cm}^2$  (low dose) and  $40 \mu\text{C}/\text{cm}^2$  (high dose), respectively, with the same EB energy (50 keV). XPS measurements were carried out to investigate interface chemistry and depth profile in a Kratos AXIS spectrometer (U.K.) with the monochromatic Al K $\alpha$  X-ray radiation at 1486.71 eV. The base vacuum in XPS analysis chamber was about  $10^{-9}$  Torr. The adhesion strength ( $G_c$ ) of the Ta/PAE interface was quantified by the four-point bending technique, which has been elaborated previously.<sup>4</sup> For each case, ten samples were tested.

To produce specimens for four-point bending testing (Fig. 1), the silicon wafer coated with the above-mentioned film stacks (Ta/PAE) were diced into rectangular pieces of sizes of  $46 \times 7$  mm and were then glued to bare silicon with an epoxy. The individual four-point bend specimens were centrally notched with a precision cutter to within  $\sim 100 \mu\text{m}$  to the thin-film interface. This is to ensure that the crack can propagate into the interfaces rather than penetrate into the massive silicon substrate.

Figure 2 gives a schematic setup for four-point bending test. The specimen is tested using four-point bending with loading rate around  $0.05 \mu\text{m/s}$ . The loads are measured to 0.01-N resolution and digitally recorded to generate the load-displacement curve. When the load is high enough, a pre-crack will initiate from the pre-notch and propagate perpendicularly toward the interface in the thin-film stack, and can grow longitudinally along the weakest interface. Mechanics of interface cracks<sup>10</sup> indicate that sufficiently far away from the pre-notch, the crack propagates along the weakest interface at a constant load, corresponding to steady propagation. The constant load ( $P_c$ ) is independent of the crack length and is related to  $G_c$  as follows<sup>10</sup>

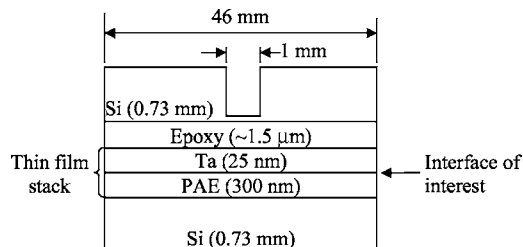


Figure 1. The Ta/PAE interface of interest.

<sup>z</sup> E-mail: ezhgan@ntu.edu.sg

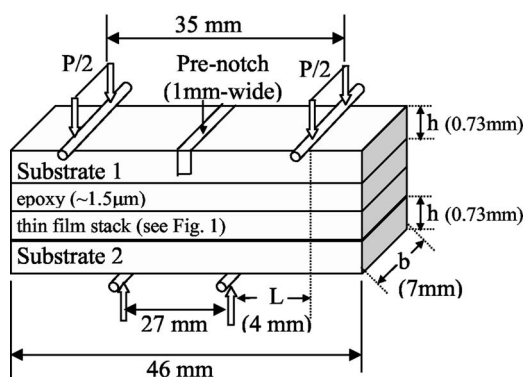


Figure 2. Schematic setup for the four-point bending test.

$$G_c = \frac{21(1 - \nu^2)P_c^2 L^2}{16Eb^2 h^3}$$

where  $E$  and  $\nu$  are the elastic modulus and Poisson's ratio of Si, respectively,  $P_c$  is the load at the plateau, and  $L$ ,  $b$ , and  $h$  are specimen dimensions shown in Fig. 2.

### Results and Discussion

**Four-point bending measurement.**—Figure 3a shows representative load vs displacement plots obtained from four-point bending adhesion test samples of Ta/PAE structures with and without EB treatment. The interfacial energy release rate ( $G_c$ ) was shown in Fig. 3b. The average  $G_c$  values obtained are  $5.9 \pm 1.1$ ,  $8.1 \pm 0.5$ , and  $4.0 \pm 0.6$  J/m<sup>2</sup> with EB doses of 0, 20, and 40  $\mu\text{C}/\text{cm}^2$ , respectively (Table I). The highest adhesion energy was observed for the case with 20  $\mu\text{C}/\text{cm}^2$  dose of EB treatment, which could be attributed to the active PAE surface induced by the EB, thus improving the Ta-PAE bonding. However, with the high-dose (40  $\mu\text{C}/\text{cm}^2$ ) EB treat-

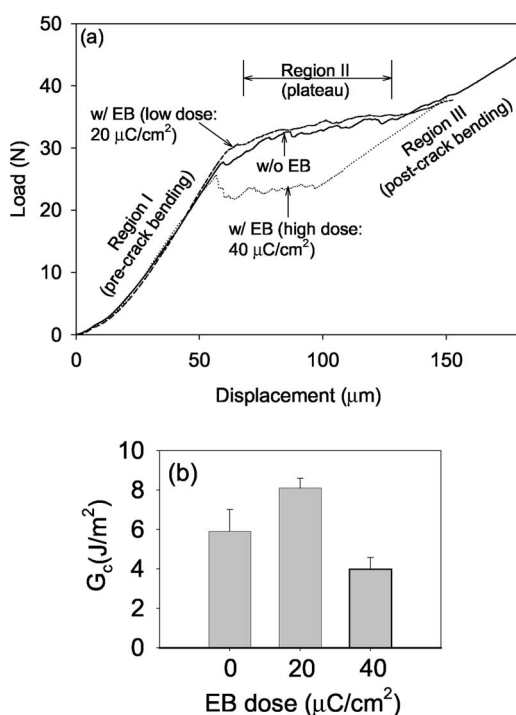


Figure 3. (a) Representative load-displacement curves for specimens with and without EB treatment. (b) The measured interfacial adhesion energy ( $G_c$ ) for three kinds of specimens.

Table I. Comparison between XPS analysis and four-point bending measurement.

|  | XPS analysis       |                                     | Four-point bending test $G_c$ (J/m <sup>2</sup> ) |
|--|--------------------|-------------------------------------|---|
|  | Max O at interface | $x$ (TaC <sub>x</sub> at interface) |   |
| wt % EB                                      | ~20%               | ~1.8                                | $5.9 \pm 1.1$                                     |
| Low-dose EB (20 $\mu\text{C}/\text{cm}^2$ )  | <5%                | ~2.3                                | $8.1 \pm 0.5$                                     |
| High-dose EB (40 $\mu\text{C}/\text{cm}^2$ ) | <5%                | ~0.2                                | $4.0 \pm 0.6$                                     |

ment,  $G_c$  value reduced by about one-third compared to the pristine case. One possible explanation may be the damage caused by the EB. However, the EB dose of 40  $\mu\text{C}/\text{cm}^2$  in our study is much lower than that of the immersing system in a conventional as-deposited EB curing process ( $\sim 500$   $\mu\text{C}/\text{cm}^2$ ).<sup>11</sup> Thus, no damage was observed under in-line field emission scanning electron microscopy (FESEM). The interfacial improvement and degradation induced by the low- and high-dose EB is further discussed, combining with the interfacial C-Ta bond information from XPS analysis.

To understand the delaminated interface, both surfaces (i.e., top and bottom) after delamination were examined by XPS survey scans. Figure 4 compares typical spectra obtained from both fractured surfaces for specimens without EB treatment and with high-dose (40  $\mu\text{C}/\text{cm}^2$ ) EB treatment. Basically, there is no clear difference between the two kinds of specimens. The peaks corresponding to C 1s and Auger, O 1s and Auger were observed at both top and bottom surfaces. These peaks should belong to the PAE film. However, at top surfaces, strong Ta 4f, 4d, and 4p peaks are also detected, confirming that the delamination took place along the Ta/PAE interface during four-point bend testing.

**XPS analysis.**—In order to understand the Ta/PAE interfacial reaction, XPS depth profile and detailed core-level spectra analysis were conducted. Figure 5 compares the XPS depth profile of Ta/PAE low- $k$  interfaces for all three cases. Tails of the Ta element are observed in the depth profiles in Fig. 5, indicating that the Ta/PAE interface is not sharply defined. A small amount of Ta atoms may diffuse into the PAE film attributed to the porous characteristic of PAE. A tail was also observed at the Ta/porous a-SiC:H interface previously.<sup>12</sup> For the pristine case (Fig. 5a), about 20% atoms located in the Ta/PAE interface are oxygen (O 1s), which is not de-

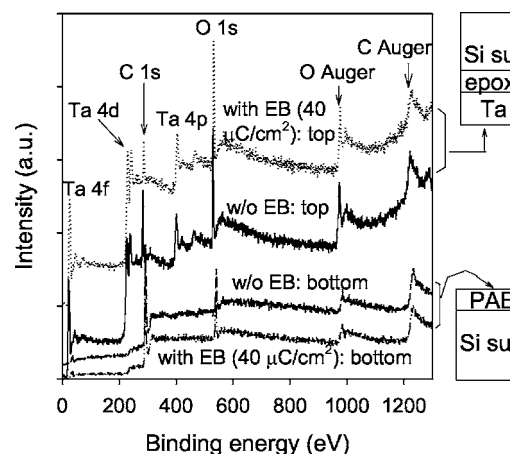
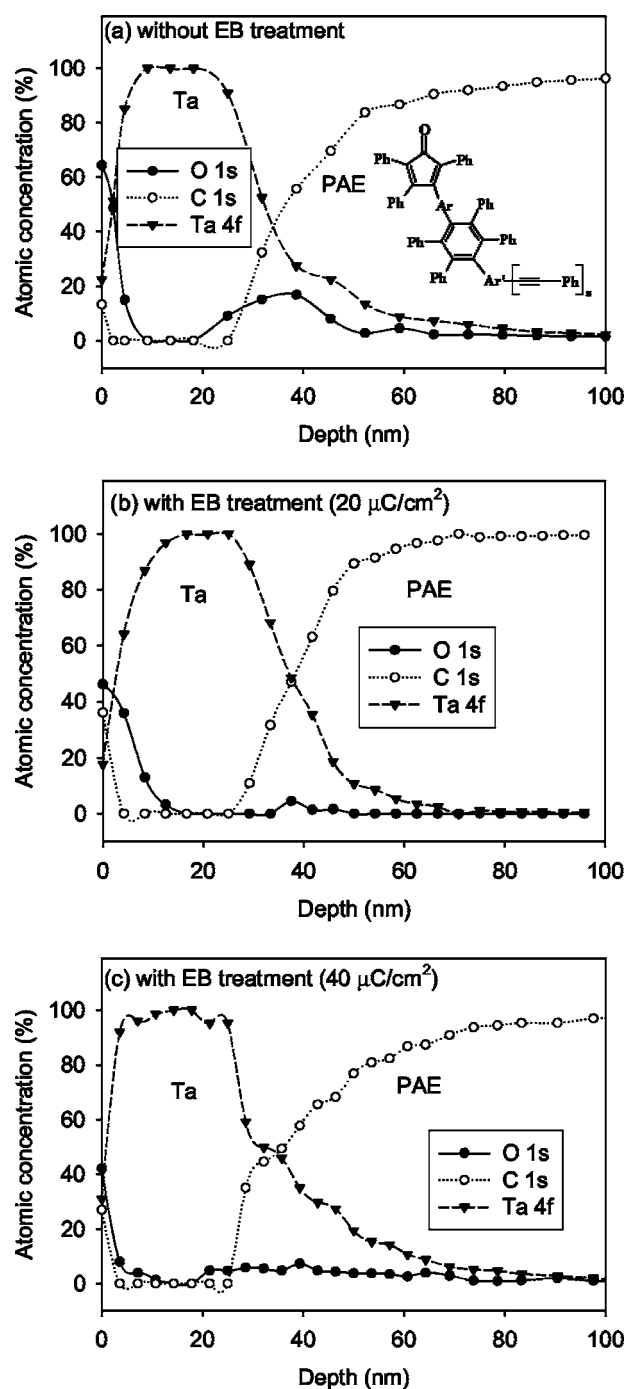
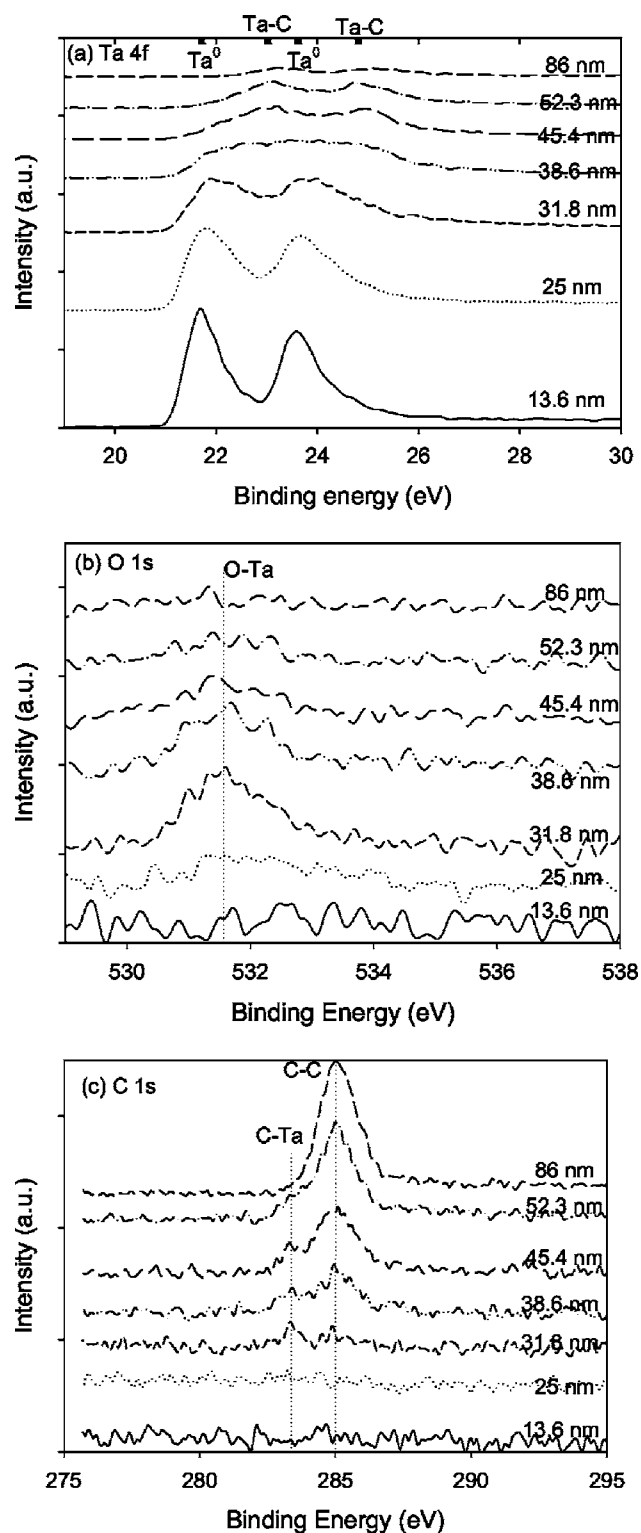


Figure 4. Typical XPS survey spectra from fractured surfaces, consisting of top and bottom parts (see schematic, not in scale). The thickness of the Si substrate, epoxy, Ta, and PAE are 0.73 mm, 1.5  $\mu\text{m}$ , 100 nm, and 300 nm, respectively.



**Figure 5.** XPS depth profile of Ta/PAE low- $k$  interface: (a) without; (b) with EB treatment ( $20 \mu\text{C}/\text{cm}^2$ ); and (c) with EB treatment ( $40 \mu\text{C}/\text{cm}^2$ ). The inset in (a) shows the chemical structure of PAE precursor, where Ar and Ph are short for aryl and phenyl, respectively.

tected in the bulk of the low- $k$  film. This interfacial oxygen may result from oxygen/moisture absorption during process transfer from PAE deposition to PVD barrier deposition. Similar XPS spectra of PAE and the incorporation of oxygen have been reported earlier.<sup>13</sup> It was reported that oxygen/moisture uptake would weaken the electrical characteristics in terms of leakage current and breakdown strength.<sup>14,15</sup> However, the oxygen species were almost removed from the Ta/PAE interface with EB treatments (Fig. 5b and c), both of which show similar depth profile. It is seen that the high-energy electrons with dose of  $20 \mu\text{C}/\text{cm}^2$  is enough to break the chemical bonding of surface-absorbed oxygen.



**Figure 6.** Details of the (a) Ta 4f, (b) O 1s, and (c) C 1s spectra with respect to different depth for pristine specimen.

Figure 6 shows the details of the Ta 4f, O 1s, and C 1s spectra with respect to different depth for the pristine specimen. It is clear that until 25-nm depth there was no O and C species but Ta only, which corresponds to the surface Ta barrier layer. As expected, with the thickness increase, the Ta 4f becomes weaker and weaker. Figure 6a shows that at depth below 25 nm, the energy peaks were located at 21.7 eV (Ta  $4f_{7/2}$ ) and 23.6 eV (Ta  $4f_{5/2}$ ), indicating metallic state

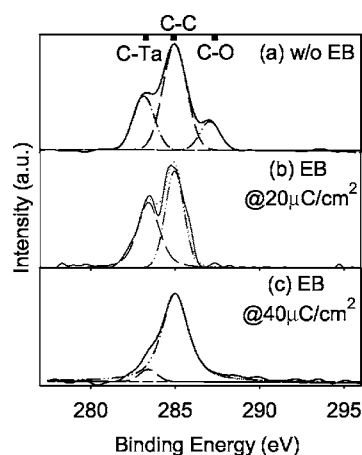


**Figure 7.** Deconvolution of C 1s spectra (a) without EB treatment, (b) with EB treatment ( $20 \mu\text{C}/\text{cm}^2$ ), and (c) with EB treatment ( $40 \mu\text{C}/\text{cm}^2$ ).

$\text{Ta}^0$ .<sup>16</sup> At depths higher than 45.4 nm, the peaks were shifted to 23.0 and 24.8 eV, respectively, which was attributed to the formation of Ta–C bonds.<sup>16</sup> At the depth in-between 25 and 45.4 nm, the composition is a mixture of metallic  $\text{Ta}^0$  and Ta–C. The oxygen atoms can be detected at the Ta/PAE interface with the highest peak at around 31.8-nm depth (Fig. 6b). No oxygen was detected in the bulk PAE film, indicating that the inherent O species in PAE film is less than the sensitivity of the XPS equipment. Therefore, a large amount of oxygen ( $\sim 20\%$ ) at the pristine Ta/PAE interface should be incorporated from the air due to processing. As observed from the C 1s spectra, at around 31.8-nm depth the peak located at 283.2 eV shows that the carbon reacts with the Ta at the Ta/PAE interface.<sup>17</sup> With the thickness increase, another peak corresponding to a C–C bond (at 285 eV)<sup>13</sup> appears and becomes stronger, which is an indication of the PAE film. It is believed that the interfacial Ta–C interaction is the key point to improve the Ta/PAE adhesion as discussed below.

To further examine the effect of EB treatment on the Ta–C interaction, Fig. 7a–c compares the spectra deconvolution of C 1s for all three cases at 38.6-nm depth. For a pristine interface (Fig. 7a), the spectrum could be deconvoluted into three components, corresponding to C–Ta bond (283.2 eV), C–C bond (285 eV), and C–O bond (287 eV), respectively. With EB treatments, regardless of the dosage applied, the C–O bond is not detectable because the absorbed O species were removed by EB (Fig. 7b and c). Compared to the pristine case (Fig. 7a), the relative amount of C–Ta bonds increased in the case with low dose EB treatment (Fig. 7b), whereas they decreased substantially in the case with high-dose EB treatment (Fig. 7c). If we consider the  $\text{TaC}_x$  compound formed at the interface, values of  $x$  are around 1.8, 2.3, and 0.2 for pristine, the low-dose, and high-dose EB treatment, respectively (Table I). This result indicated that the Ta–C interaction hardly occurred for the sample with EB (high dose). Most of the Ta atoms detected at the interface are metallic state Ta, which do not bond to C atoms. Several references have mentioned that the formation of C–Ta bonds at the interface can improve adhesion.<sup>18,19</sup> The amount of C–Ta bonds may be the main reason leading to the lower and higher adhesion energy of the specimens with the high-dose and low-dose EB treatment, respectively. Generally, the transition metals/aromatic polymers interaction is attributed to the strong charge transfer from the metal into the planar aromatic  $\pi$  system, giving high adhesion of transition metal to polymer.<sup>20</sup> It is understood here that with low dose of EB treatment, the aromatic complexes at the PAE surface are more active and more Ta–C bonds form, leading to a stronger interface. However, if too high dose of EB treatment is imposed, the aromatic complexes are locally or partially decomposed. After Ta atoms are

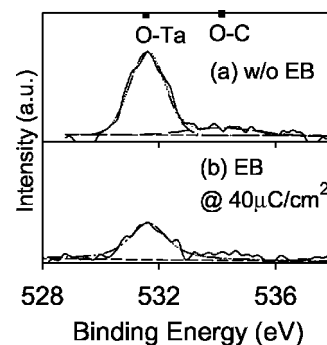


**Figure 8.** Deconvolution of O 1s spectra (a) without EB treatment and (b) with EB treatment ( $40 \mu\text{C}/\text{cm}^2$ ). Note that O 1s with EB treatment ( $20 \mu\text{C}/\text{cm}^2$ ) is not shown because it is similar to (b).

deposited on the treated polymer surface, they prefer to interact with the dangling C– bonds rather than with the whole aromatic ring, resulting in less amount of Ta–C bond formation.

Figure 8a and b clearly shows that O–Ta (at 531.5 eV)<sup>21</sup> bond densities also reduce in EB treatment cases. In other words, at the Ta/PAE interface, O–Ta bonds are also weakened if the PAE is subjected to EB treatment prior to Ta deposition. The O–Ta bond should not contribute to the interfacial adhesion strength because the oxygen absorbed onto the PAE surface is mainly caused by contamination. Thus the O–C and O–Ta bonds are weak.

It is noted that Fourier transform infrared (FTIR) spectra were taken over a wavenumber of  $400\text{--}4000 \text{ cm}^{-1}$  for pristine and EB-treated PAE films. Basically, there is no remarkable difference between these three spectra, indicating that the film structures did not show significant chemical changes after the EB treatment. EB treatment with the present dose and energy can only modify the surface of the PAE films.

## Conclusions

Porous low- $k$  is introduced with the continuous reduction of the feature sizes in ULSI. In the present study, the Ta/polymeric low- $k$  PAE interface was investigated by XPS and four-point bending test. XPS depth profile analysis shows that there is small amount of oxygen species at the interface, which was caused by contamination during film deposition. It is also found that carbon species reacted with Ta atoms to form Ta–C bonds, which contributed to the Ta/PAE interfacial adhesion. The adhesion energy ( $G_c$ ) of the Ta/PAE interface was quantitatively measured by four-point bending technique. The obtained  $G_c$  value of the pristine Ta/PAE interface was  $5.9 \pm 1.1 \text{ J}/\text{m}^2$ . If the PAE was subjected to EB treatment with low dose ( $20 \mu\text{C}/\text{cm}^2$ ) prior to Ta deposition, the adhesion energy was slightly increased to  $8.1 \pm 0.5 \text{ J}/\text{m}^2$ . However, with high-dose ( $40 \mu\text{C}/\text{cm}^2$ ) EB treatment,  $G_c$  value reduced to  $4.0 \pm 0.6 \text{ J}/\text{m}^2$ . FTIR analysis shows that the film structures did not show remarkable chemical changes after the EB treatment. XPS analysis indicated that the interfacial improvement and degradation induced by the low- and high-dose EB were correlated to the increase and decrease of the amount of C–Ta bonds at the Ta/PAE interface, respectively.

Nanyang Technological University assisted in meeting the publication costs of this article.

## References

1. International Technology Roadmap for Semiconductor (ITRS), Semiconductor Industry Association, San Jose, CA (2003).
2. M. Damayanti, J. Widodo, T. Sriharan, S. G. Mhaisalkar, W. Lu, Z. H. Gan, K. Y. Zeng, and L. C. Hsia, *Mater. Sci. Eng., B*, **121**, 193 (2005).
3. M. Damayanti, Z. H. Gan, H. S. Tan, T. Sriharan, S. G. Mhaisalkar, J. Widodo, and Z. Chen, *Thin Solid Films*, To be published.
4. C. S. Litteken and R. Dauskardt, *Int. J. Fract.*, **119/120**, 475 (2003).
5. R. H. Dauskardt, M. Lane, Q. Ma, and N. Krishna, *Eng. Fract. Mech.*, **61**, 141

- (1998).
6. M. W. Lane, E. G. Liniger, and J. R. Lloyd, *J. Appl. Phys.*, **93**, 1417 (2003).
  7. Z. H. Gan, S. Mhaisalkar, Z. Chen, S. Zhang, Z. Chen, and K. Prasad, *Surf. Coat. Technol.*, **198**, 85 (2005).
  8. P. Singer, *Semicond. Int.*, **20**, 73 (1997).
  9. T. Scherban, B. Sun, J. Blaine, C. Block, B. Jin, and E. Andideh, in *IEEE International Interconnect Technology Conference Proceedings*, pp. 257–259 (2001).
  10. P. G. Charalambides, J. Lund, A. G. Evans, and R. M. McMeeking, *J. Appl. Mech.*, **56**, 77 (1989).
  11. M. Shimada, H. Miyajima, R. Nakata, M. Yamaguchi, J. Murase, and H. Hata, *IEEE International Semiconductor Manufacturing Symposium (ISSM)*, San Jose, CA, pp. 325–328 (2001).
  12. F. Iacopi, Z. Tokei, Q. T. Le, D. Shamiryman, T. Conard, B. Brijs, U. Kreissig, M. Van Hove, and K. Maex, *J. Appl. Phys.*, **92**, 1548 (2002).
  13. A. Rajagopal, C. Gregoire, J. J. Lemaire, J. J. Pireaux, M. R. Baklanov, S. Vanhaelemeersch, K. Maex, and J. J. Waterloos, *J. Vac. Sci. Technol. B*, **17**, 2336 (1999).
  14. J. Cluzel, F. Mondon, Y. Loquet, Y. Morand, and G. Reibold, *Microelectron. Reliab.*, **40**, 675 (2000).
  15. Z. Chen, K. Prasad, Z. H. Gan, S. Y. Wu, S. S. Mehta, N. Jiang, S. G. Mhaisalkar, R. Kumar, and C. Y. Li, *IEEE Electron Device Lett.*, **26**, 448 (2005).
  16. C. J. Uchibori and T. Kimura, *J. Vac. Sci. Technol. B*, **21**, 1513 (2003).
  17. G. Gruzalski, D. M. Zehner, J. R. Noonan, H. L. Davis, R. A. Didio, and K. Muller, *J. Vac. Sci. Technol. A*, **7**, 2054 (1989).
  18. G. R. Yang, Y. P. Zhao, B. Wang, E. Barnat, J. McDonald, and T. M. Lu, *Appl. Phys. Lett.*, **72**, 1846 (1998).
  19. K. S. Kim, Y. C. Jang, H. J. Kim, Y. C. Quan, J. Choi, D. Jung, and N. E. Lee, *Thin Solid Films*, **377–378**, 122 (2000).
  20. R. Haight, R. C. White, B. D. Silverman, and P. S. Ho, *J. Vac. Sci. Technol. A*, **6**, 2188 (1988).
  21. O. Kerrec, D. Devilliers, H. Groult, and P. Marcus, *Mater. Sci. Eng., B*, **55**, 134 (1998).